# Global Mass Balance and the Length-of-day Variation

Jianli Chen

Center for Space Research, University of Texas at Austin, Austin, TX 78712, USA

E-mail: chen@csr.utexas.edu Tel: 512-232-6218, Fax: 512-471-3570

**Abstract:** Variations of atmospheric angular momentum are dominated driving forces behind the length-of-day change, while mass redistribution in the oceans and hydrosphere is expected to cause the length-of-day to change as well. We estimate atmospheric, oceanic, and hydrological contributions to the length-of-day variations during 1993 – 2004, using the National Center for Environmental Prediction reanalysis atmospheric model, the Estimating the Circulation and Climate of the Ocean consortium's data assimilating ocean general circulation model, and the US Climate Prediction Center's land data assimilation system model. A coherent mass balance among the atmosphere, ocean, and continental water is implemented. At seasonal time scales, the mass balance among the atmosphere, land, and oceans is very important, and nearly cancels all the contributions to the length-of-day variation predicted by the oceanic and hydrological models, although at intra-seasonal time scales, good correlations exist between observed length-of-day variations unaccounted for by the atmosphere and contributions from the ocean and continental water. This study indicates that in a fully mass balanced Earth system, the combined seasonal oceanic and hydrological contributions to the length-of-day variation are too small to explain the residual length-of-day variations unaccounted for by the atmosphere. The discrepancies between observed length-of-day variations and atmospheric contributions appear more likely caused by the errors of the atmospheric models, in particular of the wind fields.

**Keywords:** Earth rotation, LOD, Ocean, Hydrology, Atmospheric Angular Momentum

## 1 Introduction

At periods of a few years and shorter, the change of length-of-day (LOD) primarily results from atmospheric wind variation, while atmospheric pressure change provides important contributions as well [e.g., Barnes et al., 1983; Eubanks et al., 1988; Hide and Dickey, 1991; Gross et al., 2004]. Atmospheric angular momentum (AAM) change (i.e., combined atmospheric wind and pressure effects) accounts for about 90% of the observed LOD variability. Water mass redistribution within the oceans and continental water storage change, and associated oceanic angular momentum (OAM) and hydrological angular momentum (HAM), are also believed to play major roles in driving the residual LOD changes unaccounted for by the atmosphere. Previous studies based on various ocean models [e.g., Dickey et al., 1993; Ponte et al., 1998, 2001; Marcus et al., 1998; Johnson et al., 1999; Ponte and Ali, 2002; Gross et al., 2004] all demonstrate that the oceans provide important contributions to LOD change. However, clear quantitative understanding of oceanic effects on LOD change remains a challenging goal. A fundamental limitation is the scarcity of observations of the global oceans, which translates into relatively large uncertainties in predictions of ocean general circulation models (OGCM).

The two oceanic contributions are from variations in ocean bottom pressure (OBP) and currents, and, of these, OBP effects are probably the most difficult to estimate [e.g. Ponte and Stammer, 1999; Hu et al., 2003]. An alternative method to study oceanic mass or OBP change is the use of satellite altimeter sea surface height measurements, when steric sea surface height change, the sea surface height change caused by temperature and salinity change, and therefore, involving no mass change can be estimated and removed using independent data resource [e.g., Chen et al., 1998; Minster et al., 1999; Chen et al., 2000, 2004]. However, oceanic contributions to LOD change estimated from the TOPEX/Poseidon (T/P) satellite radar altimeter data [e.g., Chen et al., 2000b] are significantly larger than the estimates based on ocean circulation models [e.g., Johnson et al., 1999; Gross et al., 2004]. This is largely because that the T/P altimeter measures the real sea level change, and after steric effects are removed, the altimeter data represent the real mass change over the oceans. However, current ocean circulation models are not fully coupled with the atmosphere and hydrosphere, and typically employ the Boussinesq approximation to conserve total ocean volume. This will cause changes of estimated total ocean mass unrelated to any oceanographic effect. To correct this, people need to artificially force the models to conserve the total mass by adding a thin layer over the ocean [Greatbatch, 1994]. However, in the real world, the total mass of the oceans is not a constant. Mass transport among the atmosphere, land, and ocean introduces non-steric sea level change of several mm on global average, as detected by T/P altimeter data [Chen et al., 1998; Minster et al., 1999; Chambers et al., 2004].

Water storage changes over land, including changes of soil water, snow/ice sheet, and ground water are generally believed to be another major contributor to LOD change (not accounted for by the atmosphere) at seasonal time scales because of the significant seasonal cycle in the hydrosphere. A number of previous studies estimated hydrological excitations of polar motion using climatological measurements [e.g., Chao and O'Connor, 1988] and numerical climate models [e.g., Chen et al., 2000b]. Although the general conclusions are more or less the same, i.e., continental water storage change plays a major role (judged by the magnitude of the estimated excitations) in causing seasonal LOD

change, the results themselves, however do not agree with each other and the residual LOD observations (i.e., observed LOD – AAM). This is mainly limited by the lack of global measurements of related hydrological parameters (e.g., precipitation, evaportranspiration, surface runoff, soil moisture, snow water, and etc.) and the immaturity of hydrological models.

There are three major limitations in closing the total budget of LOD variations. First, atmospheric contribution is so dominant, and the residual LOD variations are highly sensitive to errors in atmospheric models, especially in the wind fields. Secondly, uncertainties in oceanic and hydrologic models are expected to be relatively more significant (than in atmospheric models) and will affect estimated oceanic and hydrologic excitations to LOD. Thirdly, and maybe most importantly, mass balance among the atmosphere, ocean, and continental water could have every significant impacts on estimated contributions from the oceans and continental water. Unlike polar motion (X, Y), the two equatorial components of the Earth rotational change, LOD variation is directly affected by the mean mass change, or the degree-0 spherical harmonics of each individual component of the earth system, e.g., the atmosphere, ocean, or continental water [Chen and Wilson, 2004]. This implies that how to implement mass balance among the atmosphere, ocean, and continental water may play a critical role in estimating atmospheric, oceanic, and hydrologic excitations to LOD change. This is the major motivation behind this study. We will assess atmospheric, oceanic, and hydrologic excitations using estimates from the National Center for Environmental Prediction (NCEP) reanalysis atmospheric model, the Estimating the Circulation and Climate of the Ocean (ECCO) consortium's data assimilating ocean general circulation model, and the US Climate Prediction Center's (CPC) land data assimilation system model. A coherent mass balance among the atmosphere, ocean, and continental water is implemented, including the mass balance between the oceans and continental water, and the mass balance between the atmosphere and the oceans and continental water combined. The main objective is to see how well the excitation budget on LOD variation can be closed, and what the main limitation is in affecting the estimates.

## 2 Theory

At a given grid point (latitude θ, longitude λ, time t), the effective LOD excitations ($\chi_3$) caused by surface mass load change ($\chi_3^{mass}$) and winds or ocean currents ($\chi_3^{motion}$) can be computed via (Eubanks 1993, Eq. A3-3, A3-4)

$$\chi_3 = \chi_3^{mass} + \chi_3^{motion}$$

$$\chi_3^{mass} = \frac{0.753 R_e^4}{C_m g} \iint \Delta P(\theta,\lambda) \cos^3\theta d\theta d\lambda \qquad (1)$$

$$\chi_3^{motion} = \frac{0.998 R_e^3}{C_m \Omega_0 g} \iiint U(\theta,\lambda) \cos^2\theta dp d\theta d\lambda$$

where Re ($6.371\times10^6$ m) is the Earth mean radius on the surface, $\Omega_0$ ($7.292115\times10^{-5}$ rad/s) the Earth mean angular velocity, g (9.81 m/s$^2$ ) the gravitational acceleration on the

Earth surface, and Cm ($7.1236 \times 10^{37}$ kg m$^2$) the principal inertia moments of the Earth's mantle. $\Delta$P and U represent atmospheric surface pressure (or OBP) and the zonal winds (or ocean currents) estimated by models. The use of numerical values from Eubanks (1993) is for consistency with our earlier results (Chen et al. 2000, 2004). We realize that the numerical values have been updated (e.g., the IERS2003 Convention), which may introduce slight change in the estimates.

Surface mass change can be represented by spherical harmonic decomposition via (Chao and Gross 1987, Wahr et al., 1998),

$$\begin{Bmatrix} \Delta C_{lm} \\ \Delta S_{lm} \end{Bmatrix} = \frac{R_e^2}{(2l+1)M} \iint \Delta\sigma(\theta,\lambda) \bar{P}_{lm}(\sin\theta) \begin{Bmatrix} \cos m\lambda \\ \sin m\lambda \end{Bmatrix} \cos\theta d\theta d\lambda \qquad (2)$$

$C_{lm}$ and $S_{lm}$ are the degree $l$ and order $m$ normalized harmonic or Stokes coefficients (of mass decomposition), $\Delta\sigma(\theta,\lambda)$ is surface mass load ($\Delta\sigma = \Delta P / g$), and M the Earth mass. $\bar{P}_{lm}$ is the $4\pi$-normalized associated Legendre function (equal to $\left[(2-\delta_{m0})(2l+1)(l-m)!/(l+m)!\right]^{1/2}$ times the ordinary associated Legendre function) (Chao 1993). The degree 2 order 0 ordinary associated Legendre functions can be expressed as (Eubanks 1993, Eq. A2-2a),

$$P_{2,0} = (3\sin^2(\theta) - 1)/2 \qquad (3)$$

and accordingly, the normalized associated Legendre functions can be computed by applying the normalization factor given above (below Eq. 2) to Eq. 3 as

$$\bar{P}_{2,0} = \sqrt{5} \cdot (3\sin^2(\theta) - 1)/2 \qquad (4)$$

To combine Eq. 1 and 4, one can derive the following relationship between surface mass excitation ($\chi_3^{mass}$) and the degree 2 and 0 zonal spherical harmonics (mass decomposition), $C_{2,0}$ and $C_{0,0}$.

$$\chi_3^{mass} = \frac{0.753 M R_e^2}{C_m} \cdot \frac{2}{3} (C_{0,0} - \sqrt{5} C_{2,0}) \qquad (5)$$

By definition $C_{0,0}$ represents the total mass change of a given component normalized by the Earth mass, $C_{0,0} = \Delta M / M$.

The above equation demonstrates that mass balance among the atmosphere, ocean, and continental water can have significant effects on estimating surface mass excitations to LOD change. Therefore, care need to be taken, when computing excitations in LOD change from each individual component. Also, any systematic bias in model estimated total mass change, such as those caused by the Boussinesq approximation in ocean circulation models, would significantly affect the results if not been corrected [Gross et al., 2004]. The $C_{0,0}$ dependence of $\chi_3^{mass}$ also possibly explains the large discrepancy between T/P altimeter estimated oceanic excitations to LOD and those from ocean circulation models, since T/P altimeter results include the $C_{0,0}$ effects, while model estimates do not.

In this study, we implement a full mass balance among the atmosphere, ocean, and continental water, in order to conserve the total mass of the atmosphere, oceans, and

continental water. We first force the ECCO ocean model to conserve total mass, then add a thin layer over the oceans equal to total water mass change over land as predicted by the CPC hydrological model. Total atmospheric mass due to changing water vapor is balanced separately by adding a uniform water layer over the land and oceans.

## 3. Data and Computation

### 3.1 Atmospheric Excitations

Atmospheric Surface pressure and wind estimates are from the NCEP reanalysis atmospheric model [Kalnay et al., 1996]. The data are provided as daily averages for the period January, 1948 to present, on a Gaussian grid, about 1.904° latitude by 1.875° longitude. The zonal winds (U) include 17 layers from the surface at 1000 mb to the top at 10 mb. Atmospheric surface pressure and wind excitations on LOD variation are computed using eq. (1). An inverted barometer (IB) correction is applied so that over the oceans, atmospheric pressure at any point is replaced by mean pressure over the oceans (not including in-land seas).

The wind integration is from the surface (defined by surface pressure) to the top of the model (10 mb). This is different from the method used to compute the NCEP AAM products archived at the Atmospheric and Environmental Research Incorporated [Salstein and Rosen 1997], in which topographic effects are neglected and the wind integration is from the lowest level at 1000 mb to the top of the model at 10 mb. As demonstrated by Aoyama and Naito (2000), including topographic effects significantly affect atmospheric wind excitations to polar motion X and Y, although effects on LOD may be insignificant.

### 3.2 Oceanic Excitations

The ECCO data assimilating OGCM is based on the parallel version of the Massachusetts Institute of Technology general circulation model and an approximate Kalman filter method [Fukumori et al., 2000]. The ECCO model (run kf049f) assimilates T/P sea surface height (SSH) observations. The model coverage is from -72.5°S to 72.5°N and has a telescoping meridional grid with a 1/3-degree resolution in the tropics (-20°S to 20°N) that gradually increases to a 1-degree resolution away from the equator. The resolution in longitude is 1 degree. There are 46 vertical levels with 10m resolution within 150m of the surface. The model is forced by NCEP reanalysis products [Kalnay et al., 1996] (12-hourly wind stress, daily heat and fresh water fluxes) with time-means replaced by those of the Comprehensive Ocean-Atmosphere Data Set. Temperature and salinity at the model sea surface are relaxed towards observed values. Model fields are available at 10-day intervals (as 10-day averages). SSH and OBP are also available at 12-hour intervals (as instantaneous values).

Following eq. (1), OBP excitations to LOD variation are computed from 12-hourly OBP estimates from the ECCO model, while ocean current excitations are based on 10-day averaged SSH and zonal (U) velocity estimates, for the period January 1993 to March 2004. The mean density of sea water (1030 $kg/m^3$) is used in current integration. The

ECCO model employs the Boussinesq approximation to conserve total ocean volume. This will cause changes of estimated total ocean mass unrelated to any oceanographic effect [Gross et al., 2004]. To correct this, we enforce ECCO mass conservation by removing a mean OBP (over the oceans) at each time step [Greatbatch, 1994]. Other mass balance corrections will be discussed in 3.4.

### 3.3 Hydrological Excitations

The CPC hydrological model is a global land surface data assimilation system [Fan et al. 2003], forced by observed precipitation, derived from CPC daily and hourly precipitation analyses, downward solar and long-wave radiation, surface pressure, humidity, 2-m temperature and horizontal wind speed from NCEP reanalysis. The output consists of soil temperature and soil moisture in four layers below the ground. At the surface, it includes all components affecting energy and water mass balance, including snow cover, depth, and albedo. Monthly average soil water storage changes are provided on a 0.5° x 0.5° grid for the period January 1980 through the present. No estimate is provided over Antarctica. The CPC soil water storage changes are estimated using the conservation equation [Vandendool, Personal Communication]. Monthly soil water data are used to compute hydrological excitations of LOD change $\chi_3$ using eq. (1), for the period January 1993 through March 2004.

### 3.4. Global Mass Balance

As mentioned above, since LOD is sensitive to the mean mass change in each individual component, a coherent mass balance needs to be considered, especially when atmospheric, oceanic, and hydrological excitations are all considered. This can be done through two steps (in addition to the mass conservation correction in the ECCO ocean circulation model). The first mass balance is between the oceans and continental water. We compute the total water storage change over the land using the monthly soil water data estimates from the CPC hydrological model, and then subtract a geographically uniform thin layer of water over the oceans equal to the total water mass change over land at each time step as predicted by the CPC hydrological model.

Another adjustment is to balance the mass between the atmosphere and a combined ocean and land system. We compute the total mass change in the atmosphere using the daily surface pressure estimates from NCEP reanalysis, and then subtract a geographically uniform thin layer of water over both the oceans and the land equal to the total mass change of the atmosphere. The excitations to LOD change from these two corrections are computed separately via eq. (1). All time series, including the computed excitations from OBP, ocean currents, continental water, and the two mass balance corrections are interpolated into the same daily intervals as the NCEP reanalysis atmospheric model, and then smoothed via a 30-day moving average before the comparison with observed LOD and atmospheric excitations.

3.5 Observed LOD Variations

LOD time series are from the International Earth Rotation and Reference Systems (IERS) combined X, Y, and LOD time series (C04), derived from various space geodetic observations. The data are daily values from September 1962 to the present. Tidal variations in LOD have been removed (http://hpiers.obspm.fr/eop-pc/analysis/excitactive.html). The daily LOD time series is smoothed via a 30-day moving average before compared with geophysical excitations.

## 4. Results and Comparison

4.1 LOD Observations and Atmospheric Excitations

The top two curves in Figure 1 show observed LOD change (the light curve) and excitations from the NCEP reanalysis atmospheric wind (surface to 10 mb) and pressure. The time series are purposely offset for clarity. The difference between observed LOD and atmospheric, or the residual LOD change unaccounted for by the atmosphere is shown in the middle of Figure 1 (light curve). The LOD residuals are apparently dominated by some long-term and decadal variations presumed to be related to core-mantle coupling. A strong 5.6-year oscillation also exists in the residual LOD change (i.e., LOD – AAM) [Abarca del Rio et al. 2000; Chen and Wilson, 2004], which is not properly explained yet. To focus the comparison on a few years or shorter time scales, we estimate the low frequency signals using a low pass filter with a cutoff frequency of 1 cycle in 4 years (shown with the dark solid curve in the middle of Figure 1). After these low frequency signals are further removed, the residual LOD change is show in the bottom of Figure 1.

The NCEP reanalysis only provides wind estimates up to 10 mb on the top of the atmosphere. However, the strength of the zonal winds in the upper atmosphere (above 10 mb) is great enough that the omission of the upper winds will have notable effects on LOD change [e.g., Rosen and Salstein, 1985, 1991; Dickey et al., 1993; Höpfner, 2001; Gross et al., 2004]. Using the seasonal amplitude and phase of upper atmospheric winds (10 mb to 0.3 mb) listed in Table 2 of Gross et al. (2004), we construct a time series for possible seasonal excitations to LOD change and show the results in the top part of Figure 2 (black curve), compared with the residual LOD change (the time series are purposely offset for clarity). It is evident that the upper winds have significant effects on the residual. The bottom curve in Figure 2 shows the LOD residual when the upper winds excitations are removed. This residual LOD time series will be used to compare with oceanic and hydrologic excitations in the following sections.

4.2 Oceanic and Hydrologic Excitations

Oceanic contribution to LOD from ECCO OBP and currents is shown in Figure 3a (red curve), while hydrological contribution from CPC is in blue. The residual LOD variation (LOD – AAM – Upper winds up to 0.3 mb) is superimposed (in gray). Based on

model estimates, both the oceans and continental water appear to play important roles in affecting the residual LOD variation, while hydrological excitations are dominated by variations at seasonal and interannual time scales, and oceanic excitations show a more broad power spectrum. Oceanic excitations follow the residual LOD time series fairly well, although the variability is significantly small. Hydrological excitations appear showing opposite phase to the rest.

The green curve in Figure 3a shows oceanic excitations when the mass balance between the ocean and land is applied, i.e. the sum of ECCO OAM and the contribution (OAM1) from adding a uniform water layer over the oceans to balance the total land water change. Apparently, this adjustment has very significant effects on oceanic excitations on LOD. When this correction is applied, oceanic excitations show significantly larger seasonal contribution to LOD, and are apparently opposite in phase to hydrological excitations.

The combined hydrological and oceanic excitations to LOD change are shown in Figure 3b, with the blue curve representing the combined excitations without land-ocean water mass balance, and the red curve with the land-ocean mass balance. After the land-ocean mass balance is applied, combined hydrological and oceanic excitations show larger seasonal component, and the interannual signals (in the blue curve in Figure 3b), originated from CPC hydrological estimates, are partly disappeared. However, when atmospheric mass is also balanced, combined hydrological and oceanic excitations, shown as the green curve in Figure 3b, virtually show no evident seasonal contributions to LOD change. This would not be a surprise if people look at individual effects (as shown in Figure 4) from the land-ocean and atmosphere and land/ocean mass balances, compared with the original hydrological and oceanic excitations estimated from CPC and ECCO. The mass balance effects are so significant and will greatly affect the estimated hydrological and oceanic excitations. There are also significant canceling effects between these individual estimates.

### 4.3 Seasonal LOD Variations

To have a clearer picture of the total budget of seasonal LOD variations, we compute annual and semiannual amplitude and phase of observed LOD change and different excitation sources using un-weighted least squares fit. The results are summarized in Table 1. Because of the strong interannual variation in observed LOD time series [e.g., Gross et al., 2004], the estimated seasonal variations of observed LOD vary with the time period chosen in the studies. The upper wind contribution significantly affects the seasonal signals in residual LOD time series. It reduces over half of the amplitude of the semiannual component (from 47.5 μs to 21.6 μs), and causes a phase difference of about 70 degree in the annual component. In a full mass balanced atmosphere, ocean, and continental water system, the amplitude of annual oceanic and hydrological excitations is only 1.4 μs, about 10% of the original model estimates.

The top panel of Figure 5 shows the phasor diagram of the annual component of residual LOD variations, and oceanic and hydrological contributions estimated from models and mass balances. Although both the ECCO ocean model and CPC hydrological model predict strong annual contribution to LOD, with comparable magnitudes to the

residual LOD change but different phases, however, imposing mass balance, especially the one between the atmosphere and land/ocean, cancels nearly all the annual contributions from model predictions. The bottom panel of Figure 5 shows the corresponding phasor diagram of the semiannual component. Oceanic and hydrological contributions, with or without mass balances applied, are too small to explain the semiannual LOD residuals. There are also significant canceling effects among individual contributions.

### 4.3 Intraseasonal LOD Variations

The top panel of Figure 6 shows Intraseasonal variations that are not accounted for by the atmosphere, compared with contributions from the oceans and continental water. The seasonal upper winds correction will not affect the Intraseasonal LOD residuals in this case. Annual and semiannual signals and other signals with periods longer than 1 year are removed from all time series. The bottom panel of Figure 6 shows the same plot as the top panel, but zooms into a 2 years period 1995 to 1996 for clarity. There are some good correlations between intraseasonal LOD residuals and effects from the oceans and continental water, although the magnitude from oceanic and hydrological contributions is significantly smaller than the observed. There is no apparent distinction between results with or without mass balance correction (s).

We estimate the cross correlation coefficients between the time series shown in Figure 6, and present the results in Figure 7. A strong peak the cross correlation coefficients at zero phase lag exists in all three cases. The maximum correlation coefficient between LOD residuals and model estimated oceanic and hydrological contributions is about 0.59, well above the 99% significance level at 0.23. When the land-ocean mass balance is imposed, this maximum correlation coefficient stays nearly unchanged (0.58), while when the full mass balance is imposed, it reduces slightly to 0.53. The land-ocean mass balance has no apparent effects on intraseasonal oceanic contribution is understandable, because, as seen in Figure 4, the land-ocean mass balance correction mainly introduces some seasonal and interannual variations. This is in part limited by the monthly sampling rate of the CPC hydrological model, and in part indicates that intraseasonal variability is relatively insignificant in current hydrological models [Chen et al., 2000b].

### 4.4 Interannual LOD Variations

As demonstrated by earlier studies [e.g. Gross et al., 2004], the atmosphere is also the dominant contributor to LOD variations at interannual time scales. Here, we look at interannual LOD residuals that are not accounted for by the atmosphere, and contributions from the oceans and continental water (see Figure 8). It should be pointed out that the long term and decadal changes and the 5.6-year oscillations have been removed (see 4.1). Before any mass balance is applied, model estimated oceanic and hydrological excitation shows some strong interannual signal that kind of follows the LOD residuals. However, after the land-ocean mass balance is applied, this interannual variability is significantly reduced, indicating that the interannual variation seen earlier mainly results from the total

water mass change over the land, and when the land-ocean mass balance is applied, it is naturally canceled out. The mass balance between the atmosphere and land/ocean again brings some apparent interannual variations to the estimated oceanic and hydrological excitations that generally follow the LOD residuals.

Figure 9 shows the cross correlation coefficients between interannual LOD residuals and contributions from the oceans and continental water. A peak of the maximum correlation coefficients at zero phase lag is evident in all three cases (see map legend on Figure 9). The two other peaks at about ± 5 years phase lag indicate that some near 5 years oscillations still exist in these time series (shown in Figure 8).

### 4.5 Coherence Spectrum Analysis

Figures 10a and b show magnitudes and phases of the coherence between LOD residuals and oceanic and hydrological excitations. Mean and trend are removed from all time series. Annual and semiannual variations have also been removed by least squares fitting. The two dashed lines in Figure 10a represent the 95% and 99% confidence level. Oceanic and hydrological excitations (with or without mass balance corrections) show good correlation with LOD residuals over much of the intra-seasonal frequency band. The two estimates without atmospheric mass balance correction show better coherence with LOD residuals from 2 to 5 cycles/year. This is consistent with the results from cross correlation analysis (see Figure 7).

## 5. Summary

Mass balance among the atmosphere, ocean, and continental water plays a critical role in computing oceanic and hydrological excitations to LOD. The results based on the NCEP reanalysis atmospheric model, the ECCO data assimilating ocean circulation model, and the CPC land data assimilation system indicate that at seasonal time scales, when mass balance is not applied, the model predicted oceanic and hydrological excitations are comparable in magnitudes to the LOD residuals unaccounted for by the atmosphere with apparent phase differences. However, when a full mass balance is applied, the seasonal oceanic and hydrological excitations become too small to explain the residual LOD changes. The mass balancing effects, especially from the balance between the atmosphere and land/ocean, nearly completely cancel the model predicted excitations.

At intraseasonal time scales, good correlations exist between the LOD residuals and contributions from the ocean and continental water. The application of mass balance among the atmosphere, ocean, and continental water does not increase the coherence between the LOD residuals and model estimated oceanic and hydrological contributions. Since the CPC model estimated global averaged continental water storage change is dominated by seasonal and longer period signals (Figure 4), the land-ocean mass balance has negligible effects on the cross correlation analysis at intraseasonal time scale. However, the NCEP reanalysis estimated atmospheric mass change does show evident power at intraseasonal frequency band. The application of atmospheric mass balance

results in an even weaker correlation. The reason is unclear. In addition, the application of the mass balance has significant effects on the estimated interannual oceanic and hydrological contributions to LOD.

This study indicates that a fully mass balance of atmosphere, ocean, and continental water is necessary when considering the global budget on LOD excitations. The estimated oceanic and hydrological excitations to LOD are highly sensitive to the mass balance corrections. The discrepancies between observed length-of-day variations and atmospheric contributions appear more likely caused by the errors of the atmospheric models, especially in the wind field. Efforts trying to closed seasonal global budget on observed LOD excitations are mainly limited by the uncertainties of atmospheric models and how to appropriately apply the mass balance(s). An ideal approach is to use model estimates from a fully coupled atmospheric, oceanic, and hydrological data assimilation system, with proper mass conservation applied.

We carry out two additional experiments to assess atmospheric mass balancing effects on LOD using different methods. One is to add a uniform layer to the surface of the oceans that has the same mass as the mass deficit of the land+atmosphere system. The other is to distribute the mass deficit of the atmosphere to the globe with a Gaussian distribution (i.e., more mass is distributed in the equatorial region), while the land and ocean are first balanced in the same way as we used in this study. The first method generates virtually the same results as what we present in this paper. However, the Gaussian distribution does show slightly larger impacts on LOD (from atmospheric mass balance), further strengthening our conclusion.

**Acknowledgments.** We would like to thank the two anonymous reviewers for their insightful comments, that led to improved presentation of the results. This research was supported by NASA's Solid Earth and Natural Hazards Program (under grants NNG04G060G, NNG04GP70G) .

**References:**

Abarca del Rio R., Gambis D, Salstein D.A., Interannual signals in length of day and atmospheric angular momentum, Annales Geophysicae, 18(3): 347-364, 2000.

Aoyama, Y., I. Naito, Wind contribution to the Earth's angular momentum budgets in seasonal variations, J. Geophys. Res., Vol. 105 (D10), 12,417-12,431, 2000.

Barnes, R., R. Hide, A. White, and C. Wilson, Atmospheric angular momentum functions, length-of-day changes and polar motion, Proc. R. Soc. Lond., A387, 31-73, 1983.

Chambers, D.P., J. Wahr, and R. S. Nerem (2004), Preliminary observations of global ocean mass variations with GRACE, Geophys. Res. Lett., 31, L13310, doi:10.1029/2004GL020461.

Chao, B.F., Gross R.S., Changes in the Earth's rotation and low-degree gravitational field induced by earthquakes, Geophys. J. Roy. Astron. Soc., 91: 569-596, 1987.

Chao, B. F., and W. P. O'Connor, Global surface water-induced seasonal variations in the Earth's rotation and gravitational field, Geophys. J. R. astr. Soc., 94, 263-270, 1988.

Chao, B. F., Geoid and its geophysical interpretation, edited by P. Vanicek and N. T. Christou, CRC Press, 285-298, 1993.

Chen, J.L., C.R. Wilson, D.P. Chambers, R.S. Nerem, and B.D. Tapley, Seasonal Global Water Mass Budget and Mean Sea Level Variations, *Geophys. Res. Lett.*, 25 (19), 3555-3558, 1998.

Chen, J.L., C.R. Wilson, B.F. Chao, B.D. Tapley, and T. Pekker, An Assessment of Hydrological Effects on Geodetic Measurements, AGU Fall Meeting, San Francisco, December 12-17, 1999.

Chen, J.L., C.K. Shum, C.R. Wilson, and D.P. Chambers, B.D. Tapley, Seasonal Sea Level Change from TOPEX/Poseidon Observation and Thermal Contribution, Journal of Geodesy, 73, 638-647, 2000a.

Chen, J.L., C.R. Wilson, B.F. Chao, C.K. Shum, and B.D. Tapley, Hydrologic and Oceanic Excitations to Polar Motion and Length-of-day Variation, G. J. Internat., Vol. 141, 149-156, 2000b.

Chen, J.L., C.R. Wilson, X.G. Hu, B.D. Tapley, Large-Scale Mass Redistribution in the Oceans, 1993 - 2001, *Geophy. Res. Lett.,* Vol. 30, No. 20, 2024, 2003.

Chen, J.L., C.R. Wilson, X.G. Hu, Y.H. Zhou, B.D. Tapley, Oceanic Effects on Polar Motion determined from an Ocean Model and Satellite Altimetry: 1993 - 2001, J. Geophys. Res., Vol. 109, No. B2, B02411 10.1029/2003JB002664, 2004.

Chen, J.L., C.R. Wilson, Interannual Variability of Low Degree Gravitational Change, 1980 - 2002, J. Geodesy, 2004 (in press).

Dickey, J.O., S.L. Marcu.; C.M. Johns, R. Hide, and S.R. Thompson, The oceanic contribution to the Earth's seasonal angular momentum budget, Geophys. Res. Lett., 20 (24), 2953-2956, 1993.

Fan, Y., Huug Van del Dool, K. Mitchell, D. Lohmann, A 51-Year Reanalysis of the U.S. land-Surface Hydrology, GEWEX News, Vol.13, No.2, Page 6-10, May, 2003.

Eubanks, T.M., J.A. Steppe, J.O. Dickey, R.D. Rosen, and D.A. Salstein, Causes of Rapid Motions of the Earth's Pole, Nature, 334, 115 - 119, 1988.

Eubanks, T.M., Variations in the orientation of the earth, in Contributions of Space Geodesy to Geodynamic: Earth Dynamics, Geodyn. Ser., vol. 24, edited by D. Smith and D. Turcotte, pp. 1-54, AGU, Washington, D.C., 1993.

Fofonoff, P. and Millard, R.C. Jr, Unesco 1983. Algorithms for computation of fundamental properties of seawater, 1983. Unesco Tech. Pap. in Mar. Sci._, No. 44, 53 pp.

Fukumori, I., T. Lee, D. Menemenlis, L.-L. Fu, B. Cheng, B. Tang, Z. Xing, and R. Giering, A Dual Assimilation System for Satellite Altimetry, Joint TOPEX/POSEIDON and Jason-1 Science Working Team Meeting, Miami Beach, Florida, 15-17 November 2000.

Greatbatch RJ, A note on the representation of steric sea level in models that conserve volume rather than mass, J. Geophys. Res., 99, 12,767-12,771, 1994.

Gross, R. S., I. Fukumori, D. Menemenlis, and P. Gegout (2004), Atmospheric and oceanic excitation of length-of-day variations during 1980–2000, J. Geophys. Res., 109, B01406, doi:10.1029/2003JB002432.

Hide, R. and J.O. Dickey, Earth's variable rotation, Science, 253, 629 - 637, 1991.

Höpfner, J. (2001) Atmospheric, oceanic, and hydrological contributions to seasonal variation in length of day, J. Geod., 75, 137-150.

Hu, X.G., J.L. Chen, B.D. Tapley, C.R. Wilson, Ocean Bottom Pressure Variability, A Study with Ocean General Circulation Models, Satellite Altimetry, and In-Situ Measurements, J. Geodesy, 2004 (in revision).

Johnson, T.J., C.R. Wilson, and B.F. Chao, Oceanic angular momentum variability estimated from the Parallel Ocean Climate Model, 1988-1998, J. Geophy. Res., 104(B11), 25,183-25,195, 1999.

Kalnay, E., et al., "The NCEP/NCAR 40-year reanalysis project," Bulletin of the American Meteorological Society, **77**, 437-471, 1996.

Marcus, Steve, Yi Chao, Jean Dickey, and Pascal Gegout, Detection and Modeling of NonTidal Oceanic Effects on Earth's Rotation Rate, Science, 1656-1659, 1998.

Minster, J.F., A. Cazenave, Y.V. Serafini, F. Mercier, M.C. Gennero, P. Rogel, Annual cycle in mean sea level from TOPEX-Poseidon and ERS-1: inference on the global hydrological cycle, *Global and Planetary Change*, **20**, Page 57-66, 1999.

Ponte, R.M., D. Stammer, and J. Marshall, Oceanic signals in observed motions of the Earth's pole of rotation, Nature, 391, 476-479, 1998

Ponte, R.M., and D. Stammer, Role of ocean currents and bottom pressure variability on seasonal polar motion, J. Geophys. Res., 104 (C10), 23,393-23,410, 1999.

Ponte, R.M., D. Stammer, and C. Wunsch, Improving ocean angular momentum estimates using a model constrained by data, Geophys. Res. Lett., 28 (9), 1775-1778, 2001.

Ponte, R.M., and A.H. Ali, Rapid ocean signals in polar motion and length of day, Geophys. Res. Lett., 29 (15), 6-1 to 6-4, 2002.

Rosen, R. D., and D. A. Salstein (1985), Contribution of stratospheric winds to annual and semi-annual fluctuations in atmospheric angular momentum and the length of day, J. Geophys. Res., 90, 8033– 8041.

Salstein, D.A., and R.D. Rosen, Global momentum and energy signals from reanalysis systems. Preprints, 7th Conf. on Climate Variations, American Meteorological Society, Boston, MA, 344-348, 1997.

Wahr, J., M. Molenaar, and F. Bryan, Time-variability of the Earth's gravity field: hydrological and oceanic effects and their possible detection using GRACE, J. Geophys. Res., 103(B12), 30,205-30,230, 1998.

**Figures:**

Figure 1. Observed LOD change, atmospheric (AAM) excitation, and residual LOD change. The top two curves are for observed LOD (light curve) and the NCEP reanalysis AAM contribution (dark curve). The middle light curve is the difference between LOD and AAM, and the dark curve represents the low frequency signals estimated from a low pass filter with a cut-off period of 4 years. The bottom curve is the LOD residuals after AAM and low frequency signals are removed.

Figure 2. Residual LOD change and upper wind (10 mb to 0.3 mb) effect. The top light curve is the residual LOD change after AAM and low frequency signals are removed, and the dark curve represents seasonal upper wind contribution from Gross et al. (2004). The bottom curve the residual LOD change after the upper wind effect is also removed.

Figure 3 a) Oceanic (OAM) and hydrological (HAM) excitations in LOD estimated from ECCO OBP and current (red curve), and CPC continental water storage change (blue curve), compared with LOD residuals (gray curves, winds up to 0.3 mb). The green curve is oceanic excitation when land-ocean mass balance is applied.

Figure 4 Combined oceanic and hydrological excitations when land-ocean mass balance is not applied (blue curve), compared with separate oceanic contribution from land-ocean mass balance (OAM1, red curve), and combined oceanic and hydrological contribution resulting from atmospheric and land/ocean mass balance (HAM2+OAM2, green curve).

Figure 5. Phasor diagrams of the (top) annual, and (bottom) semiannual components of the residual LOD variations, and of effects from the oceans, continental water, and separate contributions from land-ocean mass balance, and atmospheric or air mass balance.

Figure 6. a) Intraseasonal LOD variations (unaccounted for by the atmosphere), and oceanic and hydrological contributions during Jan. 1993 to Mar. 2004. b) Same as a), but is zoomed into a 2 years period 1995 to 1996 for clarity.

Figure 7. Cross correlation coefficients between intraseasonal LOD – AAM, and contributions from the oceans and continental water with or without mass balance(s). The dashed horizontal line represents the 99% confidence level.

Figure 8. Interannual LOD variations (unaccounted for by the atmosphere), and oceanic and hydrological contributions during Jan. 1993 to Mar. 2004.

Figure 9. Cross correlation coefficients between interannual LOD – AAM, and contributions from the oceans and continental water with or without mass balance(s). The dashed horizontal line represents the 99% confidence level.

Figure 10. a) Magnitude and b) phase of the squared coherence (for LOD) of SPACE2001 -NCEP AAM with oceanic excitations from ECCO OBP + U & V (blue curve) and T/P OBP + ECCO U & V (red curve). Annual and semiannual variations have been removed from all time series by least squares fitting. Mean and trend are also removed.

Table 1. Amplitude and phase of annual and semiannual LOD changes from space geodetic observations, atmosphere (AAM), ocean (OAM), and continental water (HAM) during the period Jan. 1993 to Mar. 2004. The phase is defined as $\phi$ in $\cos(2\pi(t-t_0)+\phi)$, where $t_0$ refers to $h^0$ on January 1.

| | Annual | | Semiannual | |
|---|---|---|---|---|
| LOD Change | Amplitude (μs) | Phase (deg) | Amplitude (μs) | Phase (deg) |
| Observed (Obs) | 353.8 | 29.6 | 258.8 | -114.9 |
| AAM (up to 10 mb) | 363.2 | 32.8 | 216.2 | -110.9 |
| AAM (up to 0.3 mb) | 343.6 | 33.6 | 243.7 | -112.2 |
| Obs - AAM (up to 10 mb) | 15.3 | -100.4 | 47.5 | -137.5 |
| Obs - AAM (up to 0.3 mb) | 18.3 | -27.8 | 21.6 | -156.9 |
| OAM | 12.4 | -159.9 | 3.5 | -149.1 |
| OAM1 (from land mass balance) | 23.4 | -130.8 | 3.3 | -127.7 |
| HAM | 17.2 | 66.7 | 6.4 | 71.6 |
| OAM+HAM | 12.5 | -247.1 | 4.4 | -257.0 |
| OAM+ OAM1+HAM (land mass balanced) | 21.1 | -162.9 | 3.5 | -208.3 |
| OAM2+HAM2 (from air mass balance) | 20.1 | 20.6 | 5.3 | -93.7 |
| OAM+HAM (Full mass balanced) | 1.4 | -228.7 | 5.0 | -132.8 |

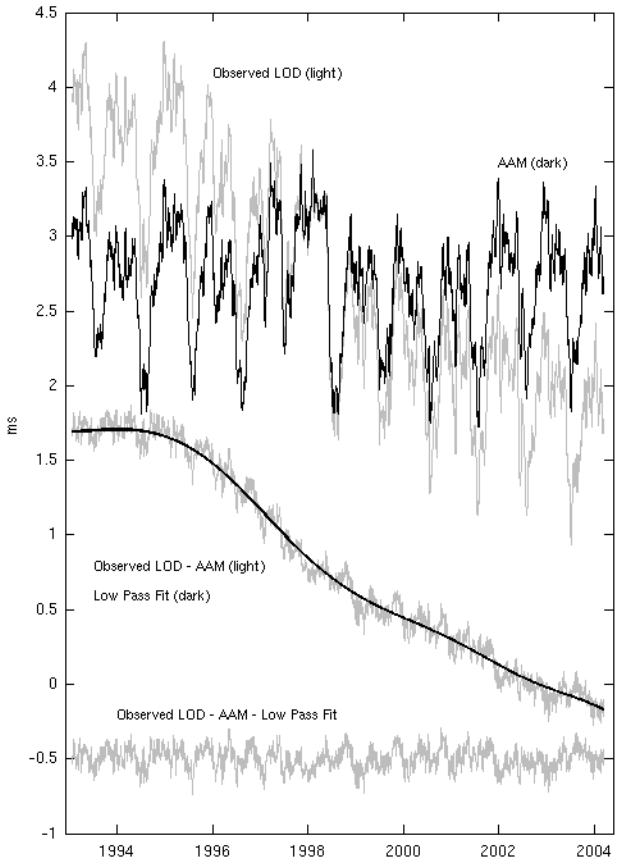
Observed LOD (light)
AAM (dark)
Observed LOD - AAM (light)
Low Pass Fit (dark)
Observed LOD - AAM - Low Pass Fit
ms
4.5
4
3.5
3
2.5
2
1.5
1
0.5
0
-0.5
-1
1994
1996
1998
2000
2002
2004

Figure 1

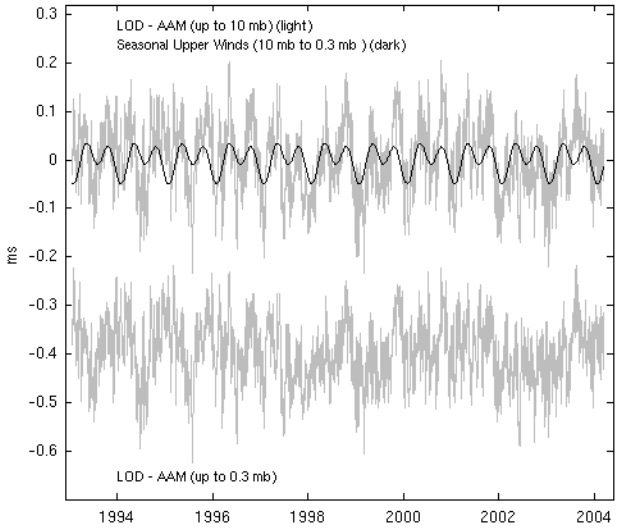


Figure 2

(a)

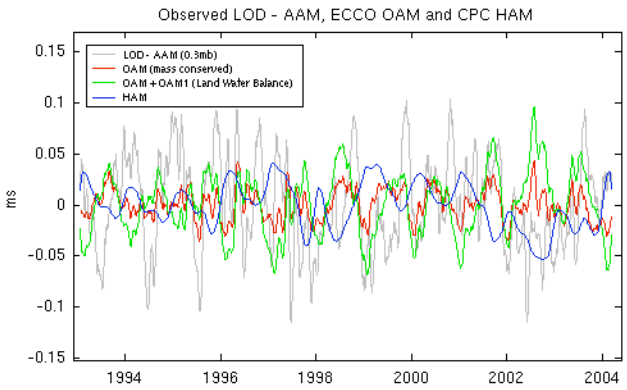


(b)

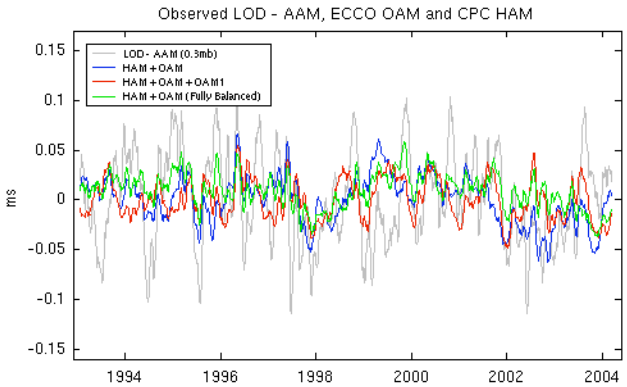


Figure 3

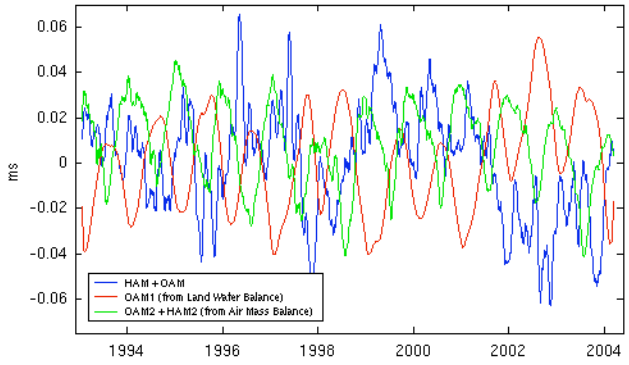


Figure 4

(a)

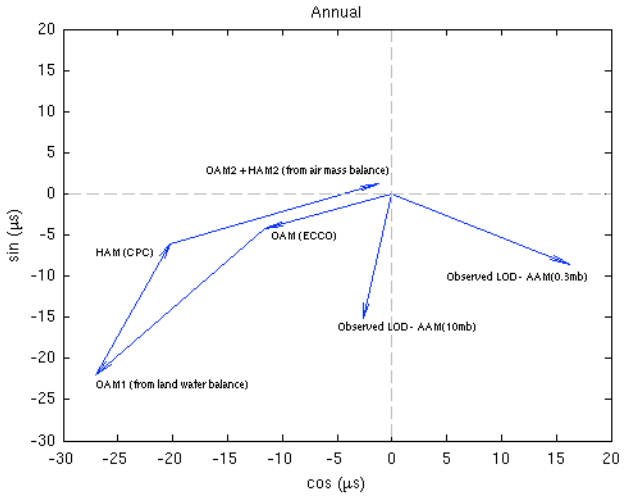


(b)

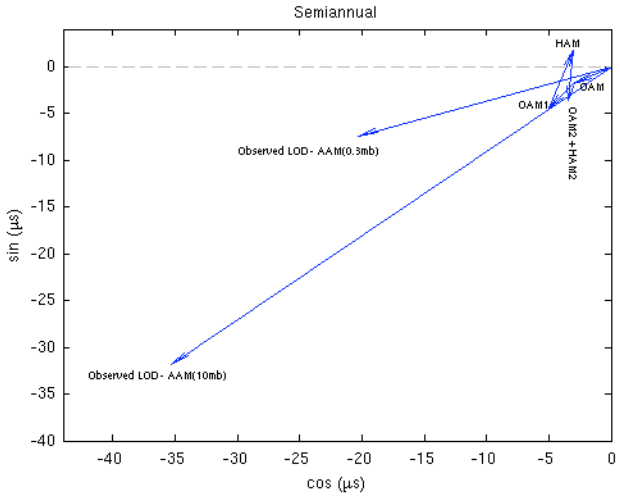


Figure 5

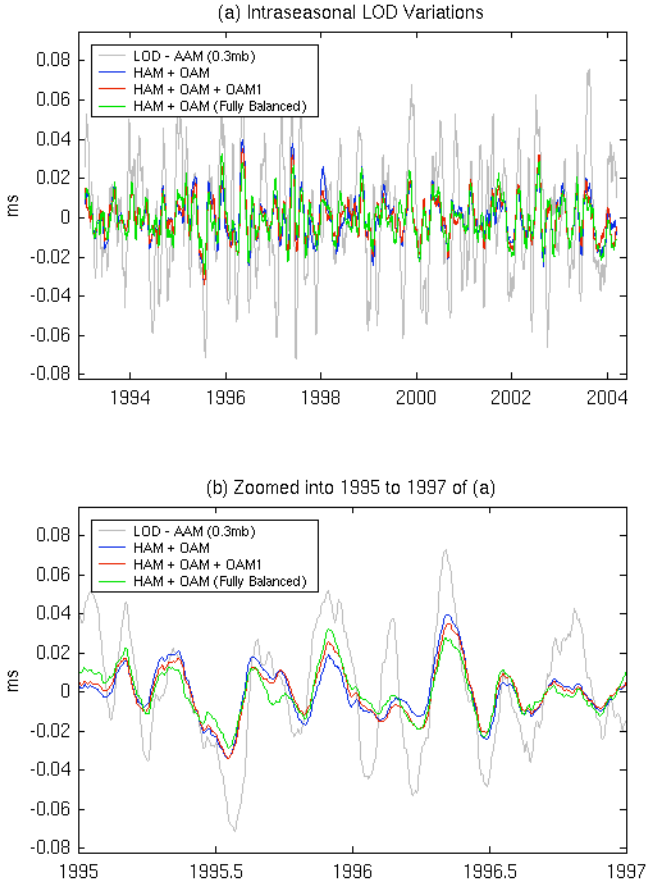
(a) Intraseasonal LOD Variations
LOD - AAM (0.3mb)
HAM + OAM
HAM + OAM + OAM1
HAM + OAM (Fully Balanced)
ms
0.08
0.06
0.04
0.02
0
-0.02
-0.04
-0.06
-0.08
1994
1996
1998
2000
2002
2004
(b) Zoomed into 1995 to 1997 of (a)
LOD - AAM (0.3mb)
HAM + OAM
HAM + OAM + OAM1
HAM + OAM (Fully Balanced)
ms
0.08
0.06
0.04
0.02
0
-0.02
-0.04
-0.06
-0.08
1995
1995.5
1996
1996.5
1997

Figure 6

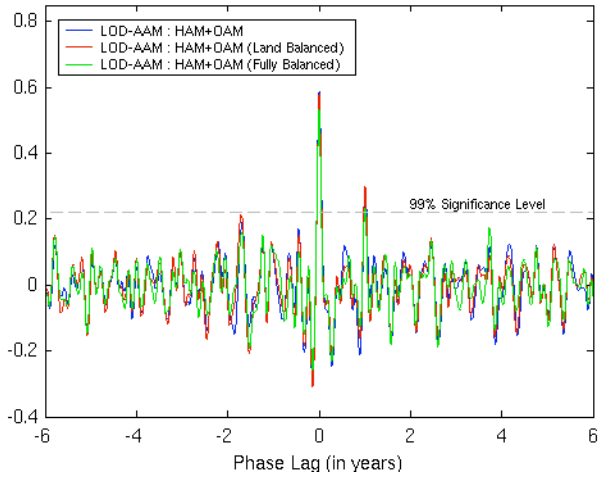


Figure 7

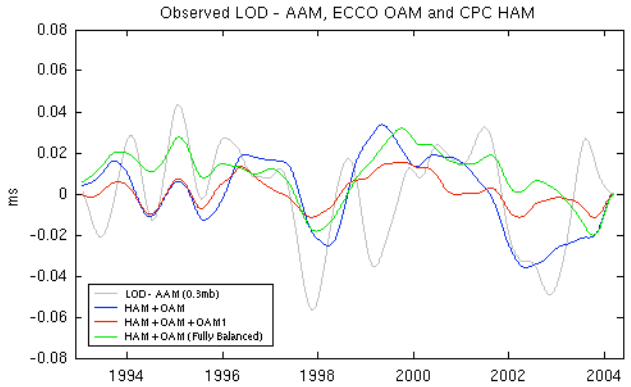


Figure 8

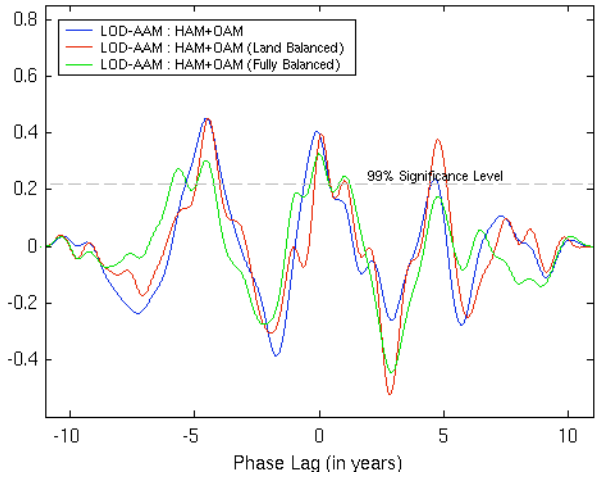


Figure 9

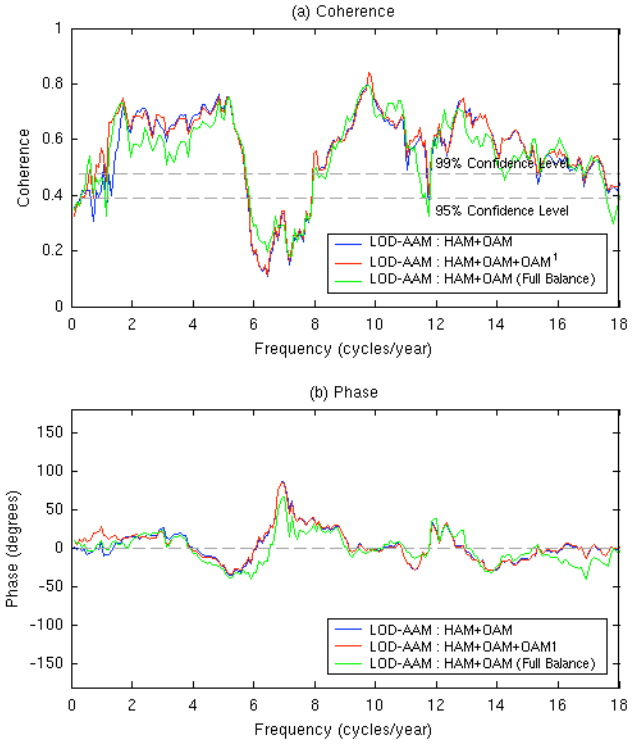


Figure 10